ACS Catalysis

pubs.acs.org/acscatalysis

Research Article

Tunable "In-Chain" and "At the End of the Branches" Methyl Acrylate Incorporation in the Polyolefin Skeleton through Pd(II) Catalysis

Chiara Alberoni, Massimo C. D'Alterio, Gabriele Balducci, Barbara Immirzi, Maurizio Polentarutti, Claudio Pellecchia, and Barbara Milani*

Cite This: *ACS Catal.* 2022, 12, 3430−3443

Read Online

ACCESS | Metrics & More | Article Recommendations | Supporting Information

ABSTRACT: The synthesis of functionalized polyolefins through coordination−insertion polymerization is a highly challenging reaction. The ideal catalyst, in addition to showing a high productivity, has to be able to control the copolymer microstructure and, in particular, the way of the polar vinyl monomer incorporation. In this contribution, we modified the typical Brookhart's catalyst by introducing in the fourth coordination site of palladium a hemilabile, potentially bidentate ligand, such as a thiophenimine (N−S). The obtained cationic Pd(II) complexes, [Pd(Me)(N−N)(N−S)][PF_6], generated active catalysts for the ethylene/methyl acrylate (MA) copolymerization leading to the desired copolymer with a different incorporation of the polar monomer depending on both the reaction medium and the N−S ligand. Surprisingly enough, the produced copolymers have the inserted acrylate both at the end of the branches (T(MA)) and in the main chain (M(MA)) in a ratio M(MA)/T(MA) that goes from 9:91 to 45:55 moving from dichloromethane to trifluoroethanol (TFE) as a solvent for the catalysis and varying the N−S ligand. The catalytic behavior of the new complexes was compared to that of the parent compound [Pd(Me)(N−N)(MeCN)][PF_6], highlighting the fact that when the copolymerization is carried out in trifluoroethanol, this complex is also able to produce the E/MA copolymer with MA inserted both in the main chain and at the end of the branches. Accurate NMR studies on the reactivity of the precatalyst [Pd(Me)(N−N)(MeCN)][PF_6] with the two comonomers allowed us to discover that in the fluorinated solvent, the catalyst resting state is an open-chain intermediate having both the organic fragment, originated from the migratory insertion of MA into the Pd−Me bond, and the acetonitrile coordinated to palladium and not the six-membered palladacycle typically observed for the Pd-α-diimine catalysts. This discovery is also supported by both DFT calculations and in situ NMR studies carried out on [Pd(Me)(N−N)(N−S)][PF_6] complexes that point out that N−S remains in the palladium coordination sphere during catalysis. The open-chain intermediate is responsible for the growth of the copolymer chain with the polar monomer inserted into the main chain.

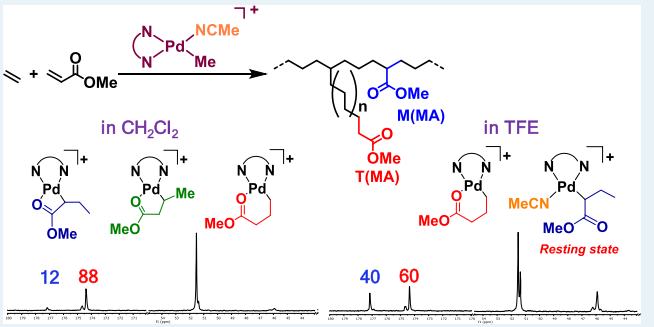

KEYWORDS: *palladium, polar vinyl monomers, copolymerization, functionalized polyolefins, microstructure, resting state*

1. INTRODUCTION

Polyolefins, such as polyethylene and polypropylene, constitute the most widespread materials in our modern society. They show an exceptional property profile that allows their application in manifold sectors, from food packaging to materials for health care, to functional textiles, to engineering plastics, etc.[1] However, at the same time, they suffer from low surface properties that are possible to improve through the introduction of polar functional groups into their otherwise nonpolar skeleton, leading to functionalized polyolefins. The presence of heteroatoms might certainly offer further different advantages, opening, as an example, to more efficient plastic degradation processes, thus facilitating their chemical recycle.[2,3] Therefore, functionalized polyolefins are highly desirable materials. However, the introduction of polar groups into the polyolefin skeleton is a challenging process and the direct, controlled, homogeneously catalyzed, copolymerization of ethylene with polar vinyl monomers represents today the most promising, environmentally friendly, and powerful approach to achieve it.[4−8]

Received: November 19, 2021
Revised: February 14, 2022

Chart 1. General Structure of a Pd Catalyst and Examples of Reported Ancillary Ligands

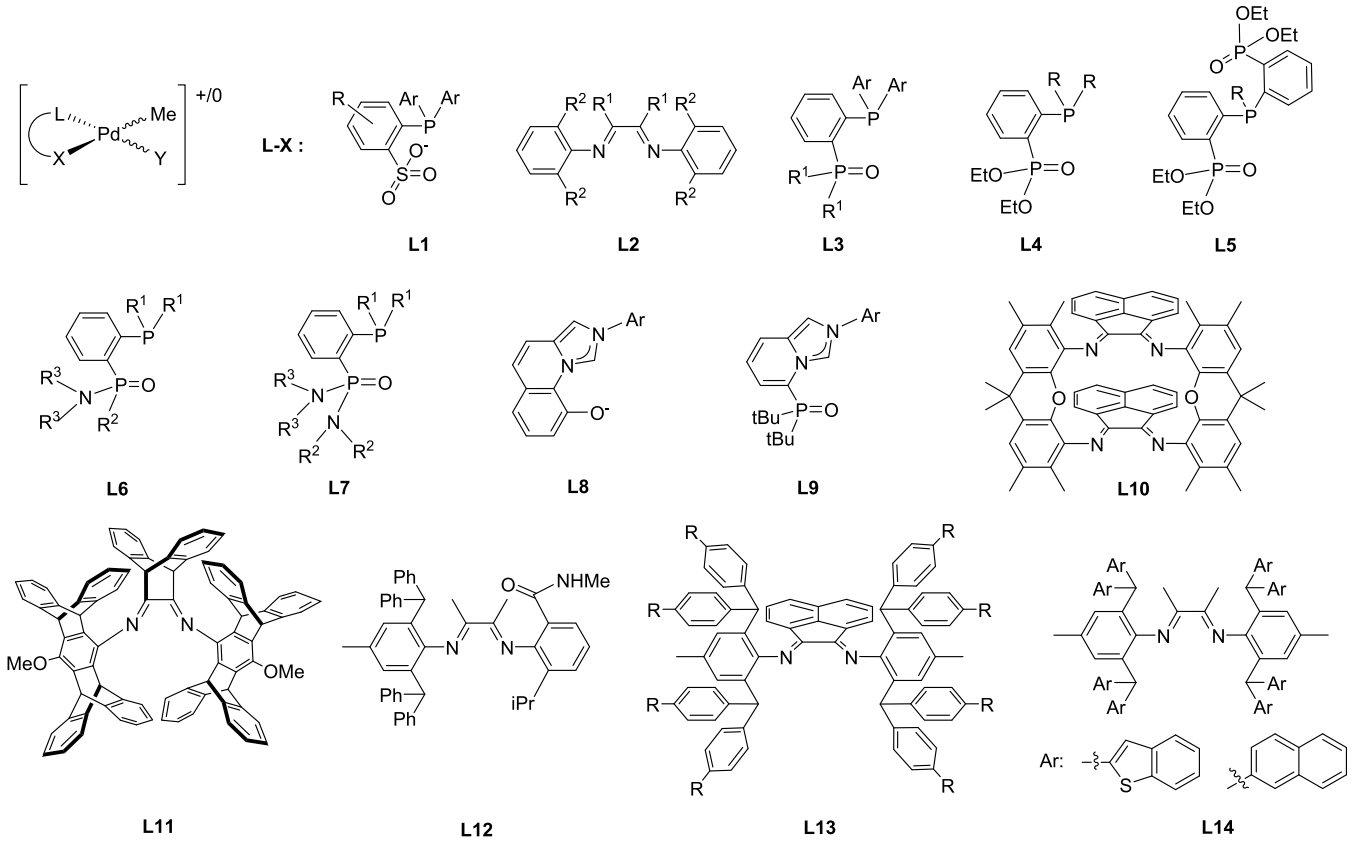

Starting from the Brookhart's pioneering work,[9,10] followed by Drent's catalytic system and its variations,[11−13] the typical homogeneous catalysts applied to this reaction are based on cationic/neutral Pd(II) complexes of general formula $[Pd(Me)(L{-}X)(Y)]^{+/0}$, having in the coordination sphere a methyl group, a bidentate ligand L−X (L = N, P, carbene C; X = N, O), and a monodentate ligand Y (Y = acetonitrile, diethyl ether, pyridine or its substituted derivatives) (Chart 1).[6]

In addition to showing a high productivity, the ideal catalyst has to be able to control macromolecular features such as molecular weight and molecular weight distribution, the amount of polar monomer incorporation, macromolecule microstructure (i.e., linear or branched polymers), and the way of polar monomer enchainment. In this context, focusing on the copolymerization of ethylene (E) with methyl acrylate (MA), the microstructure of the corresponding macromolecules is strictly related to the nature of L−X: when phosphino-sulfonate (P−O) ligands are used (**L1**, Chart 1), linear macromolecules with the polar monomer inserted into the main chain (M(MA)) are produced,[14] whereas in the case of α-diimines (N−N; **L2**, Chart 1), branched copolymers with the polar monomer at the end of the branches (T(MA)) are obtained.[15−17] Additional classes of ligands emerged in the last 10 years. As an example, chelating bisphosphine monoxide featuring diarylphosphino groups generate highly active catalysts for E/MA copolymerization leading to linear copolymers of low−moderate molecular weight, with MA randomly distributed into the main chain (**L3**, Chart 1).[18] Almost an exclusive incorporation of MA into the main chain was reported with the phosphino-(diethyl phosphonate) ligand, whereas its bis(diethyl phosphonate) counterpart leads to linear E/MA copolymers with 60% of MA into the main chain and the remaining 40% as terminating end-groups (**L4** and **L5**, respectively, Chart 1).[19] Other considered ligands are phosphine-phosphonic amide (**L6**, Chart 1)[20] and phosphine-phosphonic diamide,[21] whose palladium catalysts lead to E/MA copolymers with higher molecular weight than those obtained with P−O catalysts, and the catalyst with **L7** (Chart 1) shows also a high productivity up to 740 kg of copolymer per mol of palladium (kg CP/mol Pd).

In other few examples (**L8** and **L9**, Chart 1), ligands with NHC carbene in place of the phosphorus atom were used. The relevant palladium catalysts produce linear E/MA copolymers with moderate yields, molecular weight, and amount of the incorporated polar monomer.[22,23]

To the best of our knowledge, up to now, only two examples of Pd catalysts with α-diimines leading to E/MA copolymers with MA inserted preferentially into the main chain have been reported. In one case, the catalyst is a dinuclear complex based on a double-decker α-diimine (**L10**, Chart 1), and the trapping of the acrylic ester into the main chain is attributed to a synergistic effect between the two close palladium ions.[24] In the other, the Pd catalyst has a highly encumbered α-diimine (**L11**, Chart 1) and the incorporation of MA into the main chain is ascribed to its migratory insertion into the Pd−C bond with a primary regiochemistry instead of the secondary regiochemistry typical for catalysts with α-diimines.[25,26]

Finally, different kinds of enchainment were found in the E/MA copolymers and cooligomers produced with Ni(II) catalysts modified with pyridylimines, the macromolecular microstructure being dependent on the method of precatalyst activation.[27]

https://doi.org/10.1021/acscatal.1c05326
ACS Catal. 2022, 12, 3430−3443

Among the several tested catalysts reported in the literature, only few of them have ancillary ligands modified with specific substituents able to establish weak, secondary interactions with either palladium or ligands bonded to it. These interactions were considered to be responsible for the control of the degree of branching of the produced macromolecules. For instance, the catalyst with the amide-modified α-diimine shows a H-bonding interaction with the Pd-chlorido fragment that resulted in a higher incorporation of MA and a low degree of branching with respect to the catalyst where this group was not present (**L12**, Chart 1).[28] The branching degree was also modulated using Pd catalysts based on sterically hindered α-diimines with an acenaphthene skeleton (**L13**, Chart 1). Despite the low productivity, these catalysts led to E/MA copolymers with a low branching degree that was considered as a result of $\pi-\pi$ stacking interactions between the skeleton and one of the peripheral phenyl rings on the aryl groups.[29] The introduction of either a naphthalene or a benzothiophene group on the benzhydryl-derived α-diimine led to Pd catalysts being able to produce high molecular weight, relatively linear, semicrystalline E/MA copolymers (**L14**, Chart 1).[30]

Moreover, very recently, a paper appeared reporting that the addition of a polar additive, such as acrylonitrile, in large excess with respect to the catalyst with **L11**, resulted in lowering the branching degree in polyethylene synthesis and opened the way to the preparation of E/MA diblock copolymers.[31]

Despite the extensive research in the field, no industrial application is currently operative for the catalytic ethylene/polar vinyl monomer copolymerization reaction, which is recognized as "the polar monomer problem".[2,7]

As an alternative strategy to the largely investigated ligand design and a few other approaches applied, i.e., phase-transfer catalyst activation or redox-controlled polymerization,[32] we have now investigated the replacement of the Y ligand on the palladium coordination sphere with a hemilabile, potentially bidentate one, choosing thiopheneimines, N−S, as candidates. For this system, here, we report the effect of both the reaction medium and the hemilabile ligand on the microstructure of the obtained ethylene/methyl acrylate copolymers, together with DFT calculations and mechanistic investigations by NMR spectroscopy to shed light on the possible role played by both the solvent and N−S during the catalytic process.

2. RESULTS AND DISCUSSION

2.1. Synthesis and Characterization of Pd Complexes.

With the aim mentioned above, we have synthesized a series of palladium(II) complexes of general formula [Pd(Me)(**MeDAB**)(N−S)][PF_6] (N−S = phenyl-thiophen-2-ylmethylene-amine **1S^{Ph}**, (3,5-dimethyl-phenyl)-thiophen-2-ylmethylene-amine **1S^{Me}**, 3,5-di(trifluoromethyl)-phenyl)-thiophen-2-ylmethylene-amine **1S^{CF3}**), having coordinated to palladium both the simple α-diimine, **MeDAB**, introduced by Brookhart,[9] and a thiopheneimine (Scheme 1).

The methodology applied for the synthesis of thiopheneimines was based on the condensation reaction of 2-thiophenecarboxaldehyde with the desired aniline. In particular, **S^{Me}** was obtained by slightly modifying the literature procedure reported for the synthesis of **S^{Ph}**,[33] while **S^{CF3}** was synthesized by a new procedure based on the use of microwave irradiation. The characterized thiopheneimines (Figures S1−S9) were used to synthesize the monocationic Pd(II) complexes **1S^{Ph}**, **1S^{Me}**, and **1S^{CF3}** through a simple substitution reaction of the coordinated acetonitrile on compound

Scheme 1. Synthesis of Complexes under Investigation

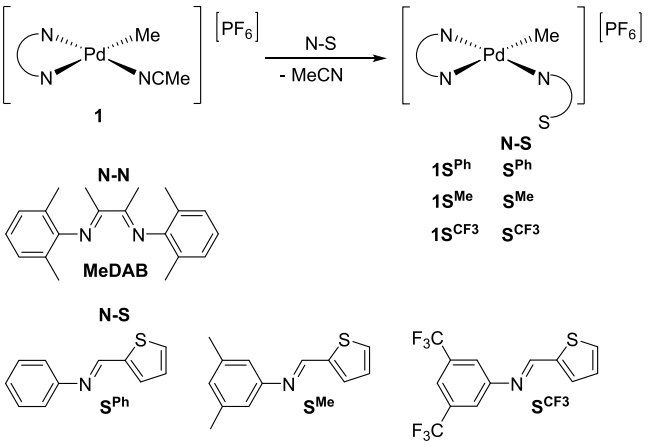

[Pd(Me)(**MeDAB**)(MeCN)][PF_6], **1** (Scheme 1). The desired complexes, isolated as yellow solids, in yields from moderate to high, were characterized in solution by NMR spectroscopy. In the ^{1}H NMR spectra, recorded in CD_2Cl_2 at room temperature (Figures S10−S21), the coordination of N−S is clearly demonstrated by: (i) the signals of its protons at chemical shifts different from those of the free ligand; (ii) the change in the resonance frequency for the protons of both **MeDAB** and Pd−Me with respect to **1**, e.g., the singlet of Pd−Me is shifted to higher frequency (from 0.34 ppm in **1** to 0.47 ppm in **1S^{Ph}**, 0.45 ppm in **1S^{Me}**, 0.47 in **1S^{CF3}**); (iii) the increased number of peaks for **MeDAB** protons due to the square planar plane not being a mirror plane any longer. In particular, the proton resonances of one of the two halves of **MeDAB** are easily assigned thanks to their remarkable shift to low frequency (from 2.22 ppm in **1** to 1.84 and 1.39 ppm in **1S^{Ph}**, 1.85 and 1.44 ppm in **1S^{Me}**, 1.86 and 1.47 in **1S^{CF3}**) due to the ring current effect of the aryl ring on the iminic fragment of N−S in cis to it. This also indicates that N−S is N-bonded to palladium. Notably, the iminic proton of N−S resonates at lower frequency with respect to the free molecule ($\Delta\delta$ = 0.32−0.23 ppm). In analogy to the palladium coordination of pyridylimines,[34−37] this shift indicates that N−S is in the *E,syn* conformation, suggesting the orientation of the sulfur atom toward palladium (Scheme 2).

Scheme 2. *E,anti* and *E,syn* Conformations for the N−S Ligand

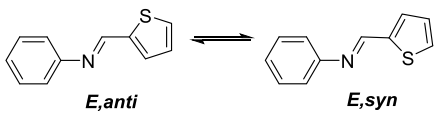

For **1S^{Ph}** and **1S^{Me}**, single crystals suitable for characterization by X-ray diffraction were obtained upon layering *n*-hexane on a CD_2Cl_2 solution of the complexes kept at 277 K for 15 days. The structure in the solid state is in agreement with the one present in solution on the basis of NMR analysis. The palladium ion has the expected square planar coordination geometry with the α-diimine acting as a chelating ligand and the thiopheneimine as a monodentate one bonded to the metal center through the nitrogen atom, whereas the sulfur atom occupies an apical position at distances of 3.100(1) and 3.328(2)/3.125(2) Å from palladium for **1S^{Ph}** and **1S^{Me}**, respectively (Figures 1a and S22, Table S1). In the case of

https://doi.org/10.1021/acscatal.1c05326
ACS Catal. 2022, 12, 3430−3443

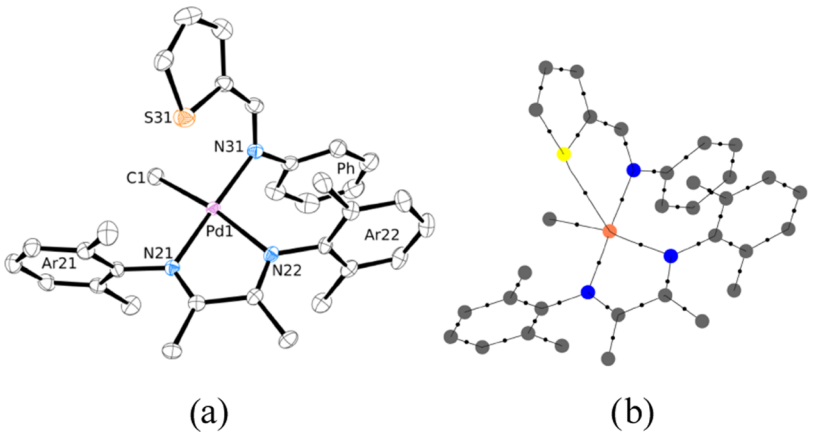

Figure 1. (a) ORTEP drawing (50% probability ellipsoids) of the molecule of $\mathbf{1S^{Ph}}$ in the crystal structure. Hydrogen atoms and the PF_6^- anion have been omitted for the sake of clarity. (b) Calculated (optimized) molecular structure of complex $\mathbf{1S^{Ph}}$ with the obtained bond paths connecting all of the nonhydrogen atoms. Black dots represent the bond critical points.

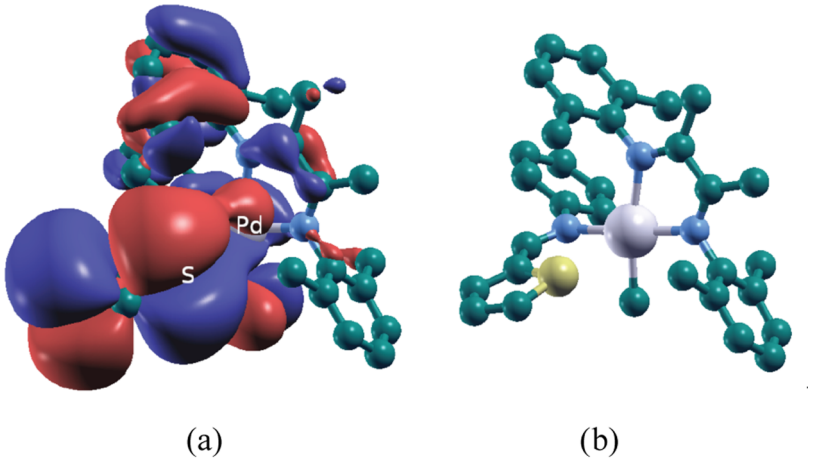

Figure 2. (a) Isosurface plot (isovalue: 3.0×10^{-5} e/Bohr^3) for the π symmetrical molecular orbital at −1.13 eV in Figure S24, which extends over both Pd and S atoms. (b) Molecular structure of complex $\mathbf{1S^{Ph}}$ with the same orientation as in panel (a), to help the reader match the isosurface to the atoms in the complex molecule.

$\mathbf{1S^{Ph}}$, a $\pi-\pi$ stacking interaction between the aryl ring of the N−S ligand and the substituted aryl of **MeDAB** *cis* to it is suggested by the pertinent geometrical parameters (dihedral angle made by the least-squares planes through the rings: 9.0°, centroid−centroid distance: 3.8 Å, centroid displacement measured on the average plane of the rings: 1.8 Å). On the other hand, in the case of $\mathbf{1S^{Me}}$, the geometrical parameters for the same intramolecular $\pi-\pi$ stacking interaction are less favorable (ring−ring dihedral angle, centroid distance, and centroid displacement—as defined above—are 16.5°, 4.3 Å, 3.3 Å, and 17.8°, 4.7 Å, 3.5 Å for the two crystallographically independent molecules, respectively), suggesting that crystal packing plays a significant role in determining this kind of weak interaction.

The Pd···S interaction in the solid state for complex $\mathbf{1S^{Ph}}$ was characterized by application of the methodology of quantum theory of atoms in molecules (QTAIM).[38] Starting from the experimental molecular structure in the solid state, a geometry relaxation was performed and the charge density of the relaxed structure was calculated in the frame of density functional theory (DFT). The topological analysis of this latter evidenced the presence of a bond path connecting Pd and S (Figure 1b). The electron density ρ_c and its Laplacian $\nabla^2\rho_c$ at the bond critical point (BCP) are 1.73×10^{-2} e/Bohr^3 and 3.85×10^{-2} e/Bohr^5, respectively, indicating a weak, closed shell, coordination interaction.[39] This is confirmed also by the contour plot of $\nabla^2\rho$ on the average plane defined by the Pd−N−thiophene moiety (Figure S23a), which shows the typical contraction of electronic charge toward the nuclei, i.e., away from the BCP, qualitatively similar to the topology of $\nabla^2\rho$ on the [N N Pd N C] equatorial plane (Figure S23b). Further evidence of the Pd···S interaction comes from the analysis of the calculated electronic structure. The projection of the density of states (DOS) onto the atomic orbitals of Pd and S shows a small but noticeable overlap of Pd-d and S-p orbitals (Figure S24), which can be further evidenced with the isosurface plot of the square modulus of the corresponding molecular orbitals (Figure 2).

This structural analysis clearly supports the presence of a weak interaction between the Pd ion and sulfur atom in the complexes under investigation.

2.2. Ethylene/Methyl Acrylate Copolymerization. Complexes $\mathbf{1S^{Ph}}$, $\mathbf{1S^{Me}}$, and $\mathbf{1S^{CF3}}$ were tested as precatalysts for the ethylene/methyl acrylate copolymerization by carrying out the reaction either in 2,2,2-trifluoroethanol (TFE) or in dichloromethane (DCM), under two sets of reaction conditions differing for the [MA]/[Pd] ratio and the ethylene pressure (P_E), referenced as set A for [MA]/[Pd] = 594 and P_E

https://doi.org/10.1021/acscatal.1c05326
ACS Catal. 2022, 12, 3430−3443

Table 1. Ethylene/Methyl Acrylate Copolymerization: Effect of N−S and the Solvent[a,b]

entry	precat.	solvent	yield (g)	kg CP/mol Pd[c]	MA (mol %)[d]	TON[e] E	TON[e] MA	M_n kDa (M_w/M_n)[f]	Bd[d,g]
1	**1**	TFE	1.3917	66.27	3.6	2095	79	24.6 (1.88)	93
2	**1S^{CF3}**	TFE	1.2608	60.04	3.2	1919	72	27.0 (2.12)	98
3	**1S^{Ph}**	TFE	0.5130	24.43	3.1	793	25	20.0 (1.64)	101
4	**1S^{Me}**	TFE	0.3521	16.77	2.9	547	16	14.7 (1.77)	103
5	**1**	DCM	0.9692	46.15	4.8	1425	72	6.0 (2.18)	90
6	**1S^{CF3}**	DCM	1.0134	48.26	4.9	1446	78	8.2 (2.11)	87
7	**1S^{Ph}**	DCM	0.7411	35.29	3.2	1141	38	10.0 (2.03)	92
8	**1S^{Me}**	DCM	0.4105	19.55	3.6	625	23	12.4 (2.00)	95

[a]Precatalyst: [Pd(Me)(MeDAB)(N-S/L)][PF_6]. [b]Reaction conditions: Set A: $n_{Pd} = 2.1 \times 10^{-5}$ mol, $V_{solvent}$ = 21 mL, V_{MA} = 1.130 mL, [MA]/[Pd] = 594, P_E = 2.5 bar, T = 308 K, t = 6 h. [c]Productivity in kg CP/mol Pd = kilograms of copolymer per mol of palladium calculated on the isolated yield. [d]Amount of inserted MA in mol % calculated by ^{1}H NMR spectroscopy on the isolated product. [e]Turnover number = mol of substrate converted per mol of Pd. [f]Determined by GPC. [g]Branching degree expressed as the number of branches per 1000 carbon atoms.

Table 2. Ethylene/Methyl Acrylate Copolymerization: Effect of N−S and the Solvent[a,b]

entry	precat.	solvent	yield (g)	kg CP/mol Pd[c]	MA (mol %)[d]	TON[e] E	TON[e] MA	M_n (M_w/M_n)[f]	Bd[d,g]
1	**1**	TFE	1.0245	48.78	4.0	1524	84	23.4 (1.19)	93
2	**1S^{CF3}**	TFE	0.9874	46.89	3.2	1519	50	30.4 (1.81)	100
3	**1S^{Ph}**	TFE	0.5509	26.23	3.4	844	30	18.0 (1.98)	98
4	**1S^{Me}**	TFE	0.3924	18.68	3.4	601	21	12.3 (1.89)	97
5	**1**	DCM	1.0380	49.43	4.8	1532	64	5.0 (2.00)	93
6	**1S^{CF3}**	DCM	0.9935	47.31	5.1	1446	78	5.4 (1.94)	93
7	**1S^{Ph}**	DCM	0.6266	29.84	4.0	943	39	11.0 (2.22)	90
8	**1S^{Me}**	DCM	0.4410	21.15	3.9	670	27	9.0 (1.89)	88

[a]Precatalyst: [Pd(Me)(MeDAB)(N-S/L)][PF_6]. [b]Reaction conditions: Set B: $n_{Pd} = 2.1 \times 10^{-5}$ mol, $V_{solvent}$ = 21 mL, V_{MA} = 2.260 mL, [MA]/[Pd] = 1188, P_E = 5 bar, T = 308 K, t = 6 h. [c]Productivity in kg CP/mol Pd = kilograms of copolymer per mol of palladium calculated on the isolated yield. [d]Amount of inserted MA in mol % calculated by ^{1}H NMR spectroscopy on the isolated product. [e]Turnover number = mol of substrate converted per mol of Pd. [f]Determined by GPC. [g]Branching degree expressed as number of branches per 1000 carbon atoms.

= 2.5 bar, and set B for [MA]/[Pd] = 1188 and P_E = 5 bar in the following. Their catalytic behavior was compared to that of the parent compound **1** (Tables 1 and 2).

All complexes generated active catalysts for the production of E/MA copolymers, isolated either as gums when the reaction was carried out in TFE, or as oils when DCM was the reaction medium. The copolymers were characterized by GPC and NMR spectroscopy to determine, respectively, the molecular weight and molecular weight distribution, and the amount of incorporated polar monomer together with the macromolecule microstructure.

In both solvents and for both sets of reaction conditions, a progressive decrease in productivity is found moving from **1** to **1S^{CF3}**, **1S^{Ph}**, and **1S^{Me}** (Tables 1 and 2). The trend inside the series of catalysts with the N−S ligand seems to be related to its coordinating capability, which is expected to increase in the same order indicating the inhibiting effect of the more coordinating ligand with respect to acetonitrile. On the other hand, decomposition to the inactive palladium metal was observed only when the reaction was carried out in dichloromethane with precatalyst **1** or **1S^{CF3}**. Thus, the higher productivity achieved in trifluoroethanol with respect to dichloromethane, under set A of reaction conditions (Table 1, entries 1 and 2 *vs* 5 and 6), is mainly due to the capability of the fluorinated solvent to stabilize the Pd−H intermediate,[40−42] which is the species of the catalytic cycle prone to evolve to palladium metal. On the other hand, the decrease in productivity found in TFE with **1** and **1S^{CF3}** moving from set A to set B of the reaction conditions (Table 1 entries 1 and 2 *vs* Table 2 entries 1 and 2) might be related to the inhibiting effect of the polar monomer that, under set B of reaction conditions, becomes more relevant due to its higher concentration. When copolymerizations were carried out with precatalysts **1S^{Ph}** or **1S^{Me}** both in TFE and DCM, no decomposition to palladium black was evident, indicating that the N−S ligand contributes to stabilize the active species. In addition, with these precatalysts, the inhibiting effect of N−S is slightly more pronounced in trifluoroethanol than in dichloromethane, as suggested by the lower productivity achieved in the fluorinated solvent (Tables 1 and 2, entries 3 and 4 *vs* 7 and 8).

The produced copolymers have M_n values in the range 5−30 kDa and rather narrow molecular weight distributions (M_w/M_n range between 1.2 and 2.2, see Tables 1 and 2). The most relevant trend is the significantly higher molecular weight of the copolymers prepared in TFE with respect to those obtained in DCM, for all of the catalysts and set of conditions. Catalyst **1S^{CF3}** in TFE affords the copolymer with the highest M_n (27.0 and 30.4 kDa under set A and set B conditions, respectively). For comparison, the same catalyst gives much lower M_n in DCM (8.2 and 5.4 kDa, see Tables 1 and 2).

The content of the inserted polar monomer is in the range 2.9−5.1 mol % (Tables 1 and 2). Regardless of the reaction conditions and the precatalyst, the copolymers synthesized in dichloromethane have a slightly higher content of methyl acrylate than those obtained in trifluoroethanol.

NMR characterization of the copolymers indicates that all of them are branched macromolecules with the degree of

https://doi.org/10.1021/acscatal.1c05326
ACS Catal. 2022, 12, 3430−3443

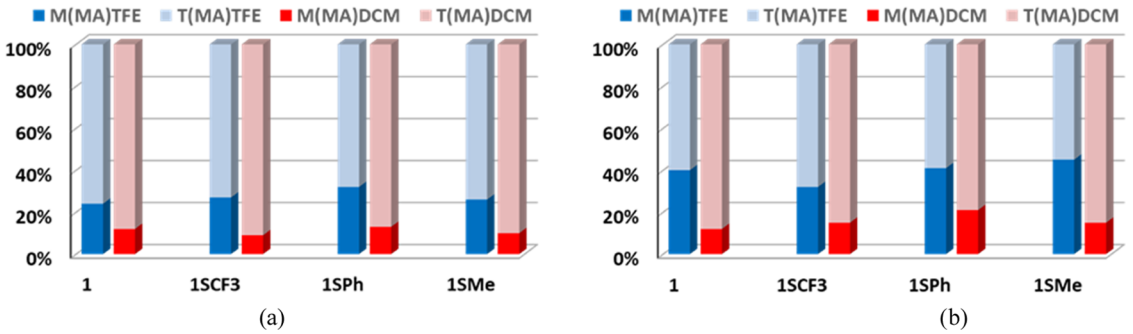

Figure 3. Ethylene/MA copolymerization: effect of the precatalyst and solvent on the way of MA enchainment as calculated by ^{13}C NMR spectroscopy on the isolated product (M(MA) = methyl acrylate in the main chain of copolymers synthesized in TFE and DCM, blue and red bars, respectively; T(MA) = methyl acrylate at the end of the branches of copolymers synthesized in TFE and DCM, light blue and light red bars, respectively). Reaction conditions: (a) Set A, Table 1and (b) Set B, Table 2.

branching in the range of 87−103 branches per 1000 carbon atoms (Tables 1 and 2). Regardless of the applied set of reaction conditions and the precatalyst, the degree of branching for the copolymers synthesized in TFE is higher than the one relative to the macromolecules produced in DCM. Moreover, the macromolecules produced in TFE with precatalysts having the N−S ligand are slightly more branched than those obtained with **1**.

The most relevant effect of both the solvent and N−S is related to the methyl acrylate enchainment. As probed by ^{13}C NMR spectra, in all of the produced macromolecules, MA is inserted both in the main chain (M(MA)) and at the end of the branches (T(MA)), with the latter prevailing (Figures 3 and S27−S30). This kind of enchainment represents a key difference with respect to the microstructure of E/MA copolymers synthesized with the reported Pd-α-diimine catalysts in dichloromethane that have the polar monomer almost exclusively at the end of the branches.[9,15]

The M(MA)/T(MA) ratio varies with the precatalyst, solvent, and set of reaction conditions. In particular, it is notable that regardless of the precatalyst and reaction conditions, a considerable increase in the percentage of M(MA) is achieved when the catalysis is carried out in trifluoroethanol with respect to dichloromethane (Figure 3, Tables S3 and S4): as an example, when **1** is used (under set B of reaction conditions), the macromolecules synthesized in TFE have M(MA)/T(MA) = 40:60, whereas for those obtained in DCM, the ratio is 12:88 (Figure 3b, Table S4).

As for the set of reaction conditions, an increase of M(MA)/T(MA) is found going from set A to set B, and the effect is more pronounced for the macromolecules produced in TFE (Figure 3a *vs* Figure 3b, Table S3 vs Table S4). In particular, in this solvent, almost a 1:1 ratio is found for the copolymers produced with $\mathbf{1S^{Me}}$ under set B of conditions (Figure 3b, Table S4). Moreover, under these reaction conditions, a clear trend of the M(MA)/T(MA) ratio with the N−S ligand is evident: the ratio increases in the order $\mathbf{1S^{CF3}} < \mathbf{1S^{Ph}} < \mathbf{1S^{Me}}$, whereas in the other cases, the highest ratio is obtained with $\mathbf{1S^{Ph}}$ (Figure 3, Tables S3 and S4). These data indicate that the peculiar enchainment of MA is due to both the solvent and N−S ligand present in the catalyst.

Focusing on precatalyst $\mathbf{1S^{Ph}}$, the effect of catalytic parameters, like temperature, precatalyst concentration, and methyl acrylate to palladium ratio, was assessed in trifluoroethanol under set A of reaction conditions. An increase in productivity, reaching the value of 79 kg CP/mol Pd, and in the amount of inserted MA—up to 5.5 mol %—was found going from 308 to 328 K, together with a decrease in the M(MA)/T(MA) ratio (Table S5). At T = 328 K, the formation of inactive palladium black was evident at the end of the reaction.

The increase of precatalyst concentration resulted in a decrease in productivity together with an increase in the content of the inserted MA (Table S6), suggesting that polynuclear species might be involved in catalyst deactivation, as we previously observed for catalysts with α-diimine ligands having a phenanthrene skeleton.[43]

In agreement with the literature,[9,10,43] the increase in the [MA]/[Pd] ratio, investigated by varying the amount of the polar monomer in the reaction mixture, resulted in a linear increase in the content of inserted MA—up to 7.9% at [MA]/[Pd] = 3782—together with a decrease in both productivity and degree of branching, and apparently a slight increase in the M(MA) to T(MA) ratio, in line with the inhibiting effect of the polar monomer (Table S7).

Complexes $\mathbf{1S^{Ph}}$, $\mathbf{1S^{Me}}$, and $\mathbf{1S^{CF3}}$ generated active catalysts also for ethylene homopolymerization, both in trifluoroethanol and dichloromethane, leading to highly branched macromolecules (Table S8). $\mathbf{1S^{CF3}}$ generated the most productive catalyst in both solvents, whereas, in analogy to what had been found in the copolymerization, productivity decreases moving to $\mathbf{1S^{Ph}}$ and $\mathbf{1S^{Me}}$, this latter being the less productive catalyst of the series in both reactions. In addition, the polyethylene produced in TFE with $\mathbf{1S^{Ph}}$, $\mathbf{1S^{Me}}$, and $\mathbf{1S^{CF3}}$ precatalysts has a degree of branching higher than the one of the macromolecules obtained with **1** (Table S8), thus suggesting that the N−S ligand affects the chain walking process.

2.3. Experimental and Theoretical Mechanistic Investigations. To shed light on the possible mechanism active for the investigated catalysts, we performed some experimental and theoretical studies using the cationic complexes **1** and $\mathbf{1S^{Ph}}$.

The reactivities of **1** and $\mathbf{1S^{Ph}}$ with both comonomers were investigated by in situ NMR spectroscopy, at room temperature, in both CD_2Cl_2 and TFE-d_3.

The first series of experiments were performed on the CD_2Cl_2 solutions of **1**. In the spectrum recorded 5 min after saturation with ethylene of a 10 mM solution of **1**, the peaks of branched polyethylene together with those of Pd-NCMe are observed, whereas no signals of the precatalyst and the gaseous monomer are present, indicating the fast conversion of **1** into

https://doi.org/10.1021/acscatal.1c05326
ACS Catal. 2022, 12, 3430−3443

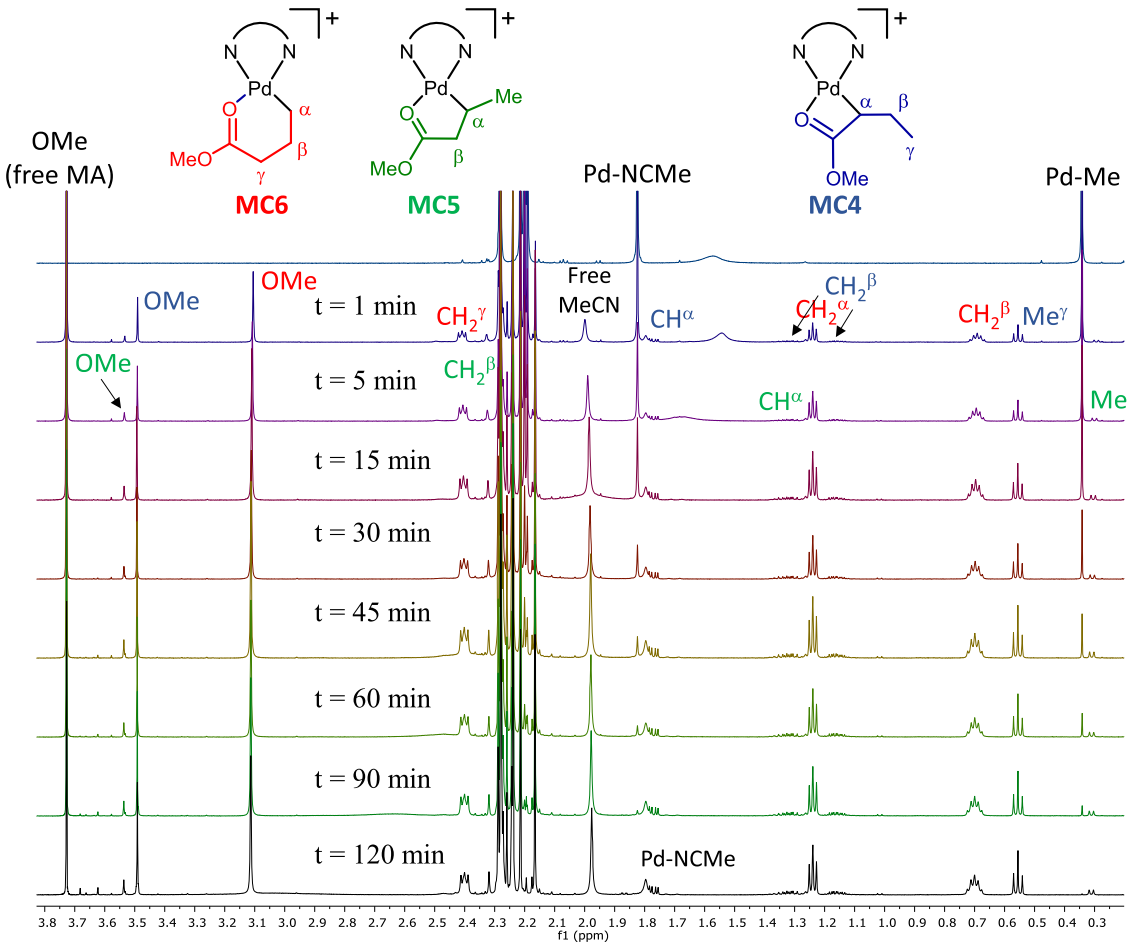

Figure 4. ^{1}H NMR spectra (CD_2Cl_2, T = 298 K) of **1** (top spectrum) and of **1** after the addition of methyl acrylate at different reaction times.

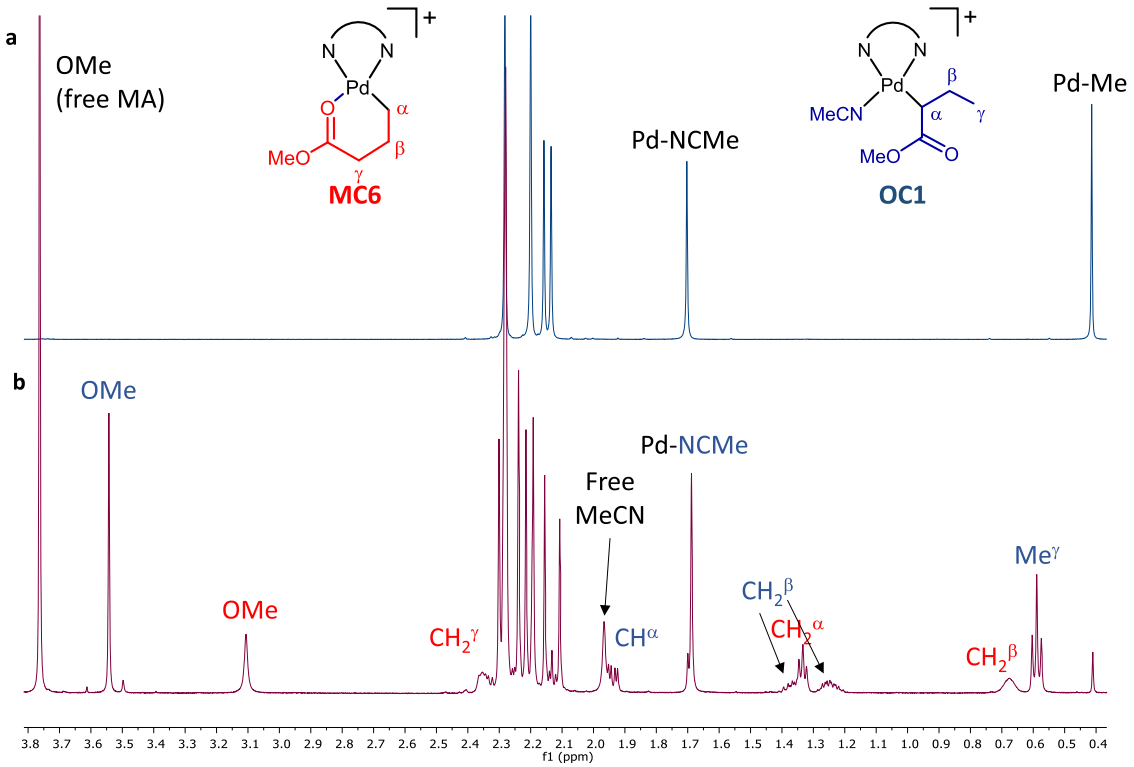

Figure 5. ^{1}H NMR spectra (TFE-d_3, T = 298 K) of **1** (spectrum a) and of **1** after the addition of methyl acrylate at (b) t = 1 min.

https://doi.org/10.1021/acscatal.1c05326
ACS Catal. 2022, 12, 3430−3443

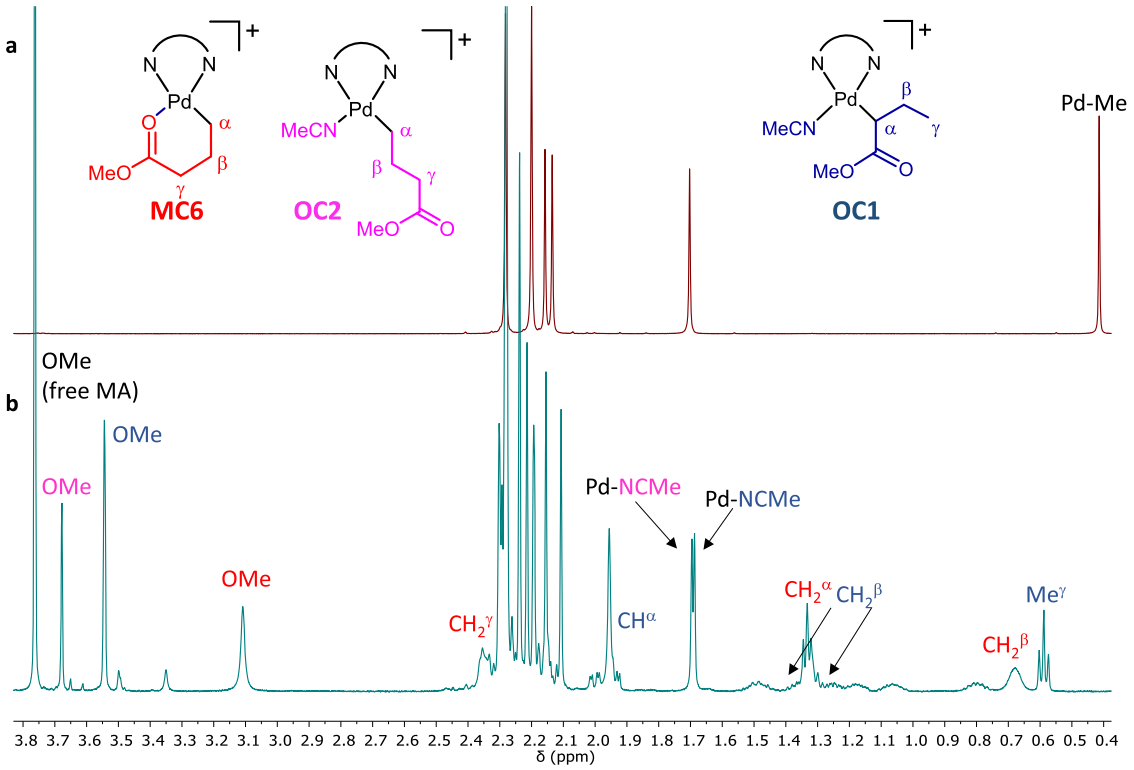

Figure 6. ^{1}H NMR spectra (TFE-d_3, T = 298 K) of **1** (spectrum a) and of **1** after the addition of methyl acrylate at (b) t = 19 h.

the active species for the homopolymerization reaction (Figures S32 and S33).

In a separate experiment, 2 equiv of methyl acrylate were added to a 10 mM solution of **1**. In the spectrum recorded after 1 min from the addition of the polar monomer, the main species is **1**, together with some intermediates resulting from the migratory insertion of MA into the Pd−Me bond. Spectral variations with time indicate the decrease of **1** that, in 2 h, is completely transformed into four-, five-, and six-membered metallacycles (**MC4**−**MC6**) that are present in the ratio 0.28:0.05:0.67 (Figures 4, S34, and S35). Unlike the typical reactivity reported for Pd-α-diimine complexes,[10,26,43−45] in this case, even the four-membered palladacycle is detected at room temperature. This metallacycle was recently observed for the first time at room temperature in analogous experiments performed on Pd-pyridyl-pyridylidene amide complexes.[46]

An additional experiment was performed by bubbling ethylene in the solution of the three metallacycles resulting in the growth of the E/MA copolymer chain. After 1 h, ethylene is consumed and no signal of free MeCN is evident (Figure S36).

The same set of experiments was performed on 10 mM solutions of **1** in TFE-d_3. The reactivity with ethylene is analogous to that observed in CD_2Cl_2: the precatalyst is immediately transformed into the active species, leading to the growth of branched polyethylene. All of the ethylene is consumed within 5 min and the signal of Pd-NCMe is clearly evident (Figure S37).

When **1** is made to react with 2 equiv of MA, two new sets of signals appear in the spectrum recorded after 1 min, in addition to those of residual **1**: one is due to the six-membered palladacycle **MC6**, and the other to a new species identified as the open-chain intermediate (**OC1**) having coordinated to the metal center both the organic fragment, resulting from the 2,1-migratory insertion of MA into the Pd−Me bond, and acetonitrile (singlet at 1.68 ppm) (Figure 5). These two intermediates are in the ratio 0.61:0.39. In this case, the reaction of **1** is completed in 30 min (Figures S38−S40). Some signals of **MC6** are broad, indicating the presence of a dynamic process in solution that, according to the exchange peak between free and bonded acetonitrile in the ^{1}H,^{1}H-NOESY spectrum, is associated with the opening−closure process of the metallacycle itself, leading to the corresponding open-chain intermediate (**OC2**) (Figure S41). The presence of **OC2** is confirmed by the resonances observed in the ^{1}H NMR spectrum recorded after 19 h (Figures 6 and S42). At this time, the solution was saturated with ethylene, resulting in the growth of the copolymer chain together with the two open-chain intermediates whose signals are still evident (Figure S42). The gaseous monomer is consumed within 15 min. The resonances of **OC1** are still present in the ^{1}H NMR spectrum recorded after 3 days, suggesting that, in the fluorinated solvent, the open-chain intermediate is the catalyst resting state (Figures S43−S45).

Analogous NMR experiments were performed on $\mathbf{1S^{Ph}}$. When a 10 mM CD_2Cl_2 solution of $\mathbf{1S^{Ph}}$ is saturated with ethylene, the signals of $\mathbf{1S^{Ph}}$, in addition to those of branched polyethylene, are observed in the spectrum recorded after 5 min (Figure S46). After 45 min, all ethylene is consumed, while $\mathbf{1S^{Ph}}$ is still present together with an increased amount of polyethylene. The solution was then saturated with ethylene once again and for further 45 min, till the consumption of the gas, and the NMR spectra showed the growth of the polyethylene chain and the presence of $\mathbf{1S^{Ph}}$. In addition, the appearance of new signals of very low intensity, in particular, a broad peak at 8.37 ppm due to the iminic proton of $\mathbf{S^{Ph}}$ bonded to the metal, indicated traces of a new palladium species. No signal assigned to free $\mathbf{S^{Ph}}$ was evident as well as no

https://doi.org/10.1021/acscatal.1c05326
ACS Catal. 2022, 12, 3430−3443

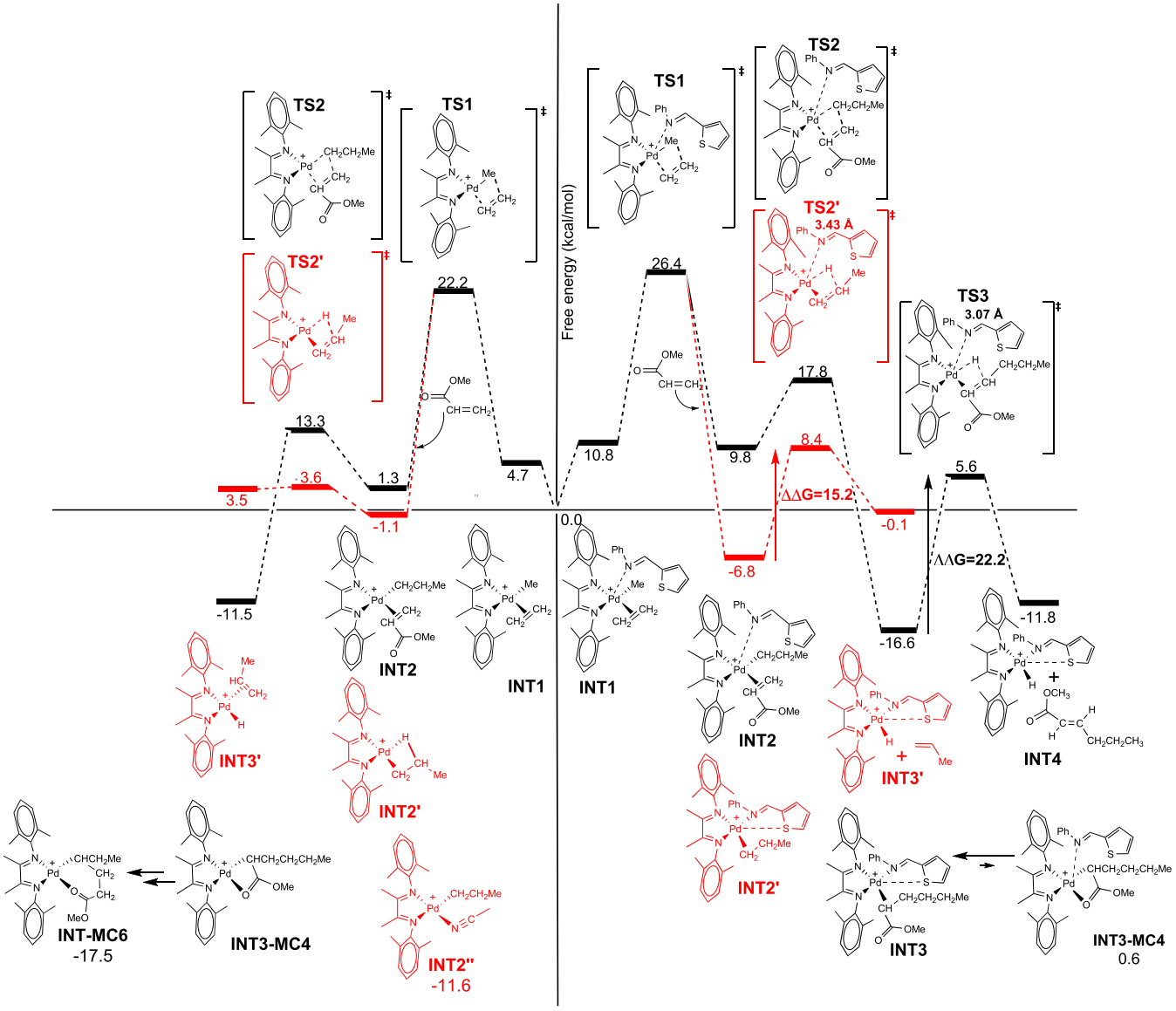

Figure 7. MEPs of the ethylene/MA copolymerization mechanism: MEP for $\mathbf{1S^{Ph}}$ (right) and MEP for **1** (left).

decomposition to the palladium metal was observed in the investigated range of time (Figure S46). Differently from the reactivity with ethylene of all of the other Pd-α-diimine complexes,[10,43,44] including **1**, these data indicate that only a very small amount of $\mathbf{1S^{Ph}}$ is transformed into the active species and that $\mathbf{1S^{Ph}}$ itself represents the catalyst resting state.

In another experiment, 2 equiv of MA were added to a 10 mM CD_2Cl_2 solution of $\mathbf{1S^{Ph}}$. No reaction was observed during the monitored time (2 h) (Figure S47), indicating again a distinctive point with respect to the reactivity of both **1** and all of the reported Pd-α-diimine complexes.[10,26,43−45]

In a third experiment, the reactivity of $\mathbf{1S^{Ph}}$, with both comonomers in the same solution, was studied by adding 2 equiv of MA to 10 mM CD_2Cl_2 solution of the complex, followed by saturation with ethylene for 5 min at room temperature. NMR spectra recorded at different reaction times evidence that the ethylene inserts first, while the signals diagnostic of MA insertion (e.g., the singlet of the methoxy group at 3.64 ppm) become evident after 45 min, together with the resonances of a new palladium complex as pointed out by the broad peak at 8.37 ppm (Figure S48). In contrast to the experiment performed with the addition of ethylene only, in this case, in the spectrum recorded after 45 min, the signal of the alkene is still present in high intensity, in agreement with the inhibiting role of the polar monomer. After 90 min, the compounds present in solution were: E/MA copolymer with MA inserted at the end of the branches, a new palladium species (broad signals at: 8.37 ppm H^{im}, 7.79 ppm H^3, and 6.69 ppm H^m), and residual $\mathbf{1S^{Ph}}$, whereas no signals of either $\mathbf{S^{Ph}}$ or metallacycle intermediates were evident (Figures S48−S50).

A final set of in situ NMR experiments was performed on the 10 mM TFE-d_3 solution of $\mathbf{1S^{Ph}}$. The reactivity with ethylene alone points out that even in the fluorinated solvent, the formation of branched polyethylene takes place immediately after the addition of the olefin (Figure S52). In addition to the signals of $\mathbf{1S^{Ph}}$, those of the new palladium species, similar to those observed in CD_2Cl_2, are evident already in the spectrum recorded after 5 min from the bubbling of ethylene. The comparison of the reactivity experiments in the two solvents points out that in the fluorinated alcohol, a higher amount of $\mathbf{1S^{Ph}}$ is transformed into the active species ($\mathbf{1S^{Ph}}$/new species = 0.87:0.13 in CD_2Cl_2 at 45 min, $\mathbf{1S^{Ph}}$/new species = 0.45:0.55

https://doi.org/10.1021/acscatal.1c05326
ACS Catal. 2022, 12, 3430−3443

Scheme 3. Proposed Mechanism for the Ethylene/Methyl Acrylate Copolymerization with 1 in DCM

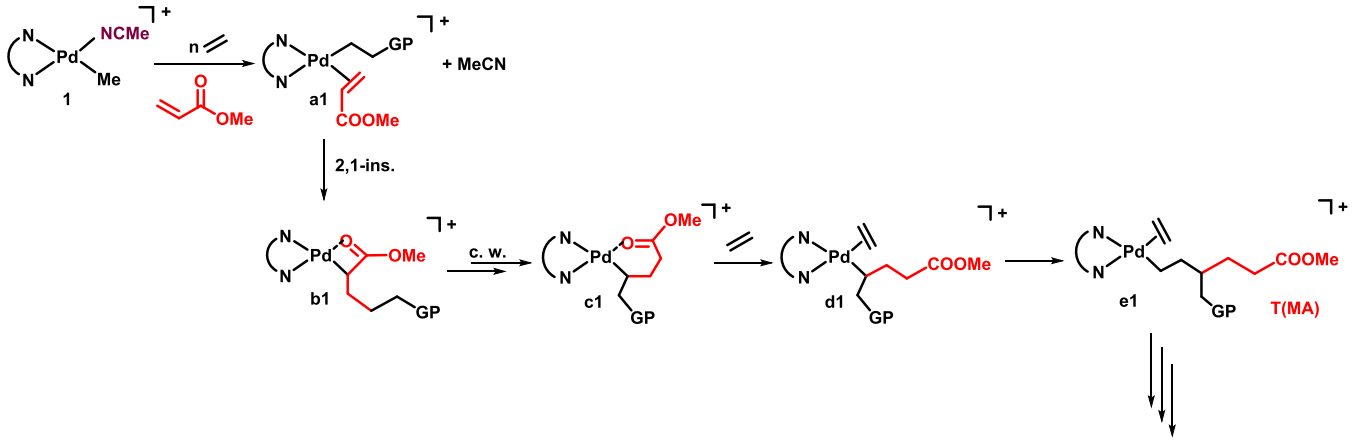

in TFE at 55 min, as calculated from the integrals of the relevant iminic proton signal).

In agreement with the experiment performed in CD_2Cl_2, even in TFE-d_3 when 2 equiv of MA was added to the solution of **1S^{Ph}**, no reaction took place within 2 h (Figure S53).

Finally, the reactivity of **1S^{Ph}** with both comonomers in the same TFE-d_3 solution was studied. The spectral variations with time indicate that even in the fluorinated solvent, the activation of the precatalyst is made by the reaction with ethylene, the insertion of MA taking place only afterward (Figure S54). But, in contrast to the reactivity in CD_2Cl_2, all ethylene is consumed within 45 min in TFE-d_3 despite the presence of MA, and after saturation of the solution with more ethylene, the copolymerization reaction proceeds further. After a total time of 2 h, the observed signals indicate the presence in solution of the growing copolymer chain, of residual **1S^{Ph}**, and of the new palladium species in a ratio with **1S^{Ph}** higher than that found in the reactivity in CD_2Cl_2 (**1S^{Ph}**/new species = 0.70:0.30 in CD_2Cl_2 at 2 h, **1S^{Ph}**/new species = 0.30:0.70 in TFE-d_3 at 2 h, as calculated from the integrals of the relevant iminic proton signal).

A series of bidimensional NMR experiments were performed to characterize the species present in solution. The ^{1}H, ^{13}C-HSQC spectrum (Figure S55) clearly indicates that the additional resonances with respect to the peaks of **1S^{Ph}** are due to a species having both **MeDAB** and **S^{Ph}** bonded to palladium. In the ^{1}H,^{1}H-NOESY spectrum (Figures S56 and S57), cross-peaks are evident among the resonances of protons of **S^{Ph}** bonded to palladium and the peak of the growing copolymer chain at 1.32 ppm, thus demonstrating that the new species is a palladium intermediate with **MeDAB**, **S^{Ph}**, and the growing chain, all bonded to the metal center. The broadness of the signals is in agreement with the presence of dynamic processes that might involve the exchange of the donor atoms of both bidentate ligands with the incoming monomers to allow the growth of the macromolecule together with the possible formation of pentacoordinated transient species. The presence of dynamic processes in a solution of $[Pd(N{-}N)_2(Me)][PF_6]$ complexes, with N−N = 1,10-phenanthroline and its substituted derivatives, was demonstrated,[47] and it was considered one of the reasons for the high productivity of $[Pd(N{-}N)_2][PF_6]_2$ complexes in CO/vinyl arene polyketone synthesis.[40]

Moreover, in the ^{1}H,^{1}H-NOESY spectrum (Figure S58), the cross-peak between the singlet of the residual OH of TFE-d_3 and the peak of a methoxy group at 3.61 ppm assigned to MA inserted into the growing polymer chain bonded to palladium indicates their close spatial relationship. This evidence strongly supports the hypothesis that the methoxy group and, reasonably, the oxygen atom of the carbonyl of MA are engaged in hydrogen bonding interactions with the fluorinated solvent and, thus, are less available for the formation of the metallacycle species involved in the chain walking process.

The main steps of the copolymerization mechanism were modeled by DFT calculations and the minimum energy paths (MEPs) for complexes **1S^{Ph}** (bearing the thiopheneimine ligand in the *E,syn* conformation) and **1** (bearing the acetonitrile) are reported in Figure 7, right and left, respectively. The zeros of our calculations are the mono-cationic complexes (**1S^{Ph}** or **1**) and the reactants at infinite distances. The reaction starts via **INT1** where ethylene is η^2-coordinated to palladium. Through **TS1**, ethylene is inserted into the Pd−Me bond. This is the rate-limiting step of both MEPs and for **1** it is 4.2 kcal/mol lower than for **1S^{Ph}**. These data are in good agreement with the experimentally observed lower productivity of **1S^{Ph}** (Tables 1 and 2) and with the results of the in situ NMR experiments. From **TS1**, two intermediates are generated, **INT2′** (in red) and/or **INT2** (in black), with MA η^2-coordinated to palladium. From this point, the reaction path splits, and we report the path leading to the β-H elimination on the propyl chain in red and the one related to the copolymerization in black. Proceeding from **INT2′**, β-H elimination of propene takes place through **TS2′** leading to the Pd−H intermediate, **INT3′**, which is slightly more stable for **1S^{Ph}** than for **1**, in agreement with the experimental observation that no decomposition to palladium black is observed for the catalysis carried out with **1S^{Ph}** in both solvents (Tables 1 and 2). This step costs 10.5 kcal/mol less for **1** than for **1S^{Ph}**. In addition, according to the in situ NMR reactivity of **1** with ethylene, the intermediate having the propyl chain and acetonitrile coordinated to Pd, **INT2″**, is at −11.6 kcal/mol.

Moving to the copolymerization mechanism (black path), starting from **INT2**, MA inserts into the Pd−C bond of the propyl chain with secondary regiochemistry, through **TS2** and this step for **1** is 4.5 kcal/mol lower than for **1S^{Ph}**, in agreement with the inhibiting effect of the N−S ligand and with the in situ NMR experiments. Different intermediates are obtained depending on whether **1** or **1S^{Ph}** is considered. For **1**, in agreement with the literature,[10,26,43−45] the four-membered palladacycle **INT3-MC4** is the product that evolves to the

https://doi.org/10.1021/acscatal.1c05326
ACS Catal. 2022, 12, 3430−3443

Scheme 4. Proposed Mechanism for Ethylene/Methyl Acrylate Copolymerization with 1 in TFE

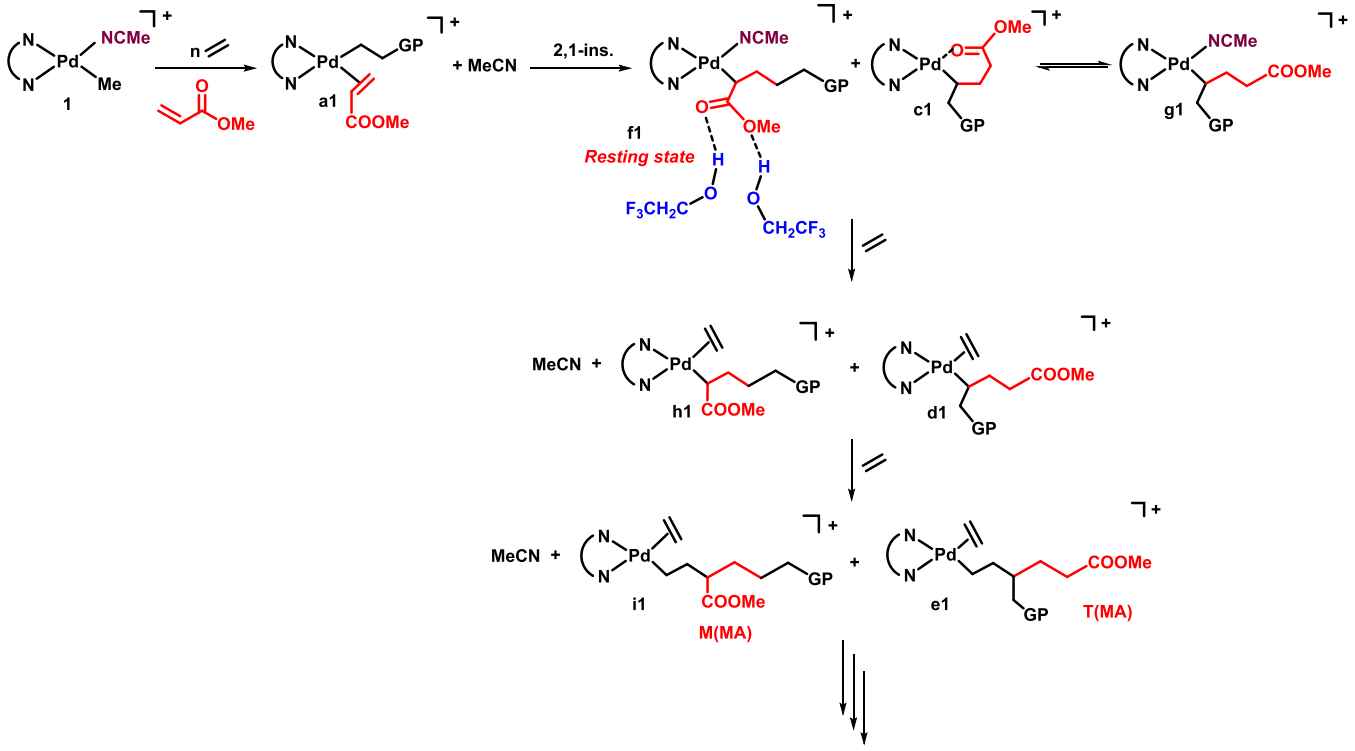

more stable six-membered cycle **INT-MC6** that is recognized as the resting state of the catalysis when the reaction is carried out in DCM as the solvent. In the case of $\mathbf{1S^{Ph}}$, **INT3** with the open methylhexenoyl chain coordinated to palladium is formed. This intermediate is more stable than both the corresponding **INT3-MC4** and all of the other possible metallacycles (Table S9, Chart S1). This data is in agreement with the in situ NMR studies about the reactivity of $\mathbf{1S^{Ph}}$ with both MA and ethylene where no signals due to the metallacycles were detected. From **INT3**, β-H elimination of *E*-methyl hex-2-enoate takes place through **TS3** leading to the Pd−H intermediate, **INT4**. This step has an energetic barrier higher than that for the β-H elimination of propene taking place through **TS2′** ($\Delta\Delta G$ = 22.2 kcal/mol *vs* 15.2 kcal/mol). This data correlates well with the formation of a branched copolymer having MA also into the main chain and not only at the end of the branches. Thus, from this analysis, it is clear that the thiopheneimine ligand can tune the main processes leading to chain walking. In particular, by comparing the Pd···N distances in the relevant **TS2′** and **TS3**, we can see that the lower the distance, the higher the barrier. In addition, the shorter Pd···N distance in **TS3** than in **TS2′** (3.07 *vs* 3.43 Å, respectively) might be related to the higher electrophilicity of the methylhexenoyl chain in **TS3** than the propyl chain in **TS2′** that results in a stronger Pd···N interaction of the thiopheneimine ligand and allows us to discriminate the rate of the chain walking process if it takes place after the insertion of ethylene or after the insertion of MA.

Intermediates **INT-MC6** and **INT3** can undergo multiple insertion reactions of the comonomers, but their analysis exceeded the scope of this preliminary investigation.

Overall, by combining the NMR data resulting from the reactivity of **1**, or $\mathbf{1S^{Ph}}$, with the two comonomers and DFT calculations, it is possible to depict the mechanism of the copolymerization reaction (Schemes 3−5). In agreement with the higher binding affinity of palladium for ethylene than MA,[10] both **1** and $\mathbf{1S^{Ph}}$ are activated through the migratory insertion reaction of ethylene into the Pd−Me bond, followed by multiple insertions of ethylene. When the insertion of the polar monomer takes place, the mechanism differs depending on the precatalyst and the solvent used as the reaction medium.

When the acetonitrile derivative **1** is used in dichloromethane as the solvent, the coordination/migratory insertion of MA into the growing chain leads to the four-membered palladacycle **b1** that, through the chain walking process, evolves to the six-membered metallacycle **c1**, which, in turn and following the typical pathway of the α-diimine catalysts, yields the fragment of the copolymer chain with MA at the end of branches **e1** (Scheme 3).

When **1** is used in trifluoroethanol, the intermediates resulting from the migratory insertion reaction of MA are both the six-membered palladacycle **c1** and the open-chain intermediate with coordinated acetonitrile **f1**, the latter being the new resting state of the catalytic cycle (Scheme 4). The formation of **f1**, as well as other open-chain intermediates (e.g., **g1**), might be favored by a network of hydrogen bonds among trifluoroethanol and the oxygen atoms of the ester group of inserted MA, as suggested by the above-discussed ^{1}H,^{1}H-NOESY experiment (Figure S58). The growth of the copolymer proceeds on both the open-chain intermediates and the metallacycle leading to macromolecules having the polar monomer in the main chain and at the end of the branches.

When the copolymerization is catalyzed by $\mathbf{1S^{Ph}}$ in dichloromethane, the highly preferred incorporation of MA at the end of the branches indicates that the copolymerization proceeds following the typical pathway of the Pd-α-diimine catalysts with the difference that the N−S ligand remains in close proximity to the metal center (Scheme 5 left). On the

https://doi.org/10.1021/acscatal.1c05326
ACS Catal. 2022, 12, 3430−3443

Scheme 5. Proposed Mechanism for the Ethylene/Methyl Acrylate Copolymerization with $1S^{Ph}$

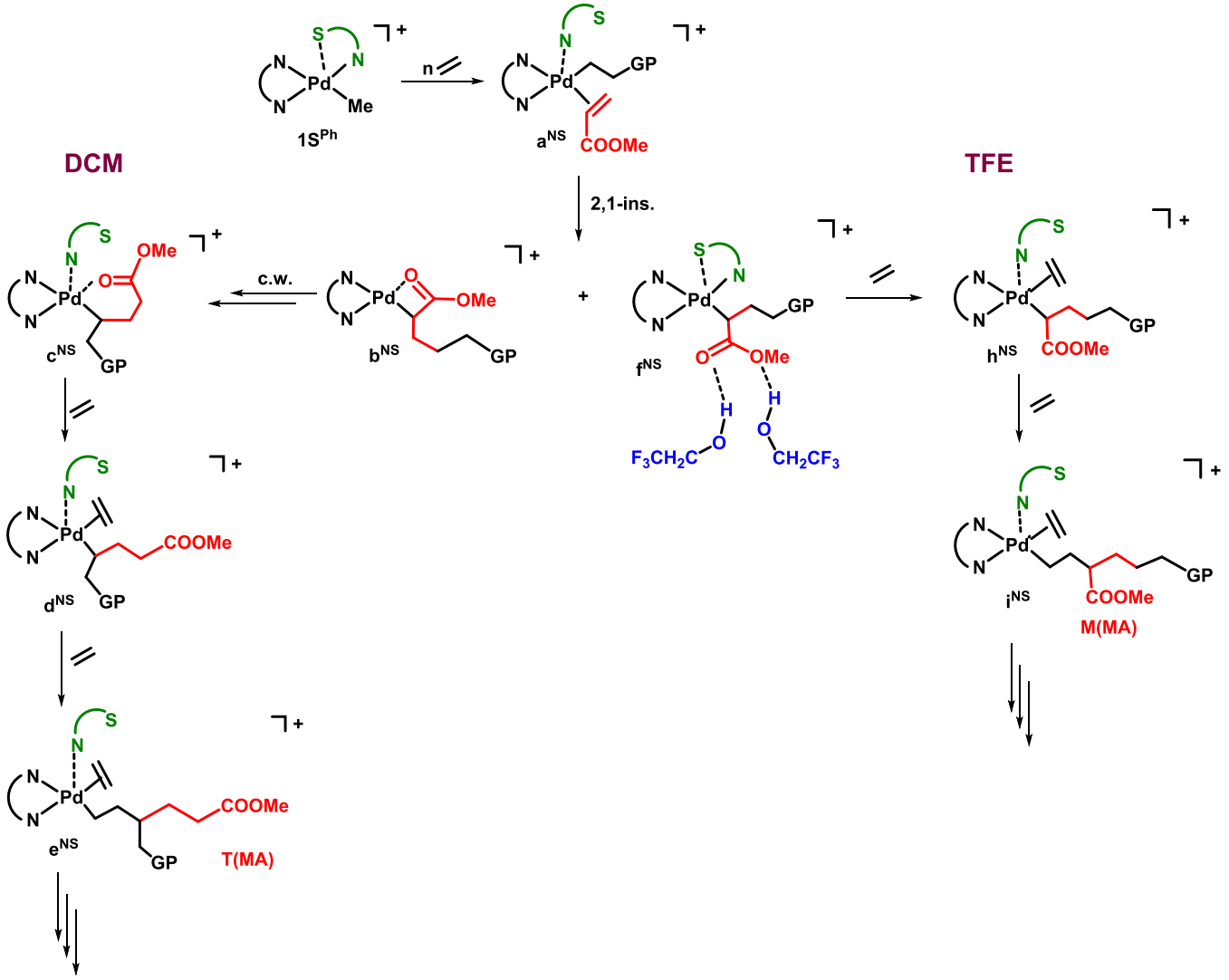

other hand, when the copolymerization is carried out in trifluoroethanol, the presence of M(MA) in the produced macromolecules and the results of both NMR reactivity studies and DFT calculations indicate that the open-chain intermediate with N−S coordinated, $\mathbf{f}^{NS}$, should be present in the catalytic cycle. Coordination and insertion of ethylene on $\mathbf{f}^{NS}$ leads to the growth of the copolymer chain with MA in the main chain (Scheme 5 right).

3. CONCLUSIONS

In summary, we have investigated a series of organometallic, cationic Pd(II) complexes, [Pd(Me)(**MeDAB**)(N−S)][PF_6], having the methyl-substituted α-diimine (**MeDAB**) and a thiophenimine (N−S) in the metal coordination sphere. Their characterization, both in the solid state and in solution, highlights that the thiophenimine acts as a hemilabile, potentially bidentate ligand, being coordinated to palladium through the iminic nitrogen atom and having the sulfur atom pointing to the metal in an apical position. Both X-ray structure analysis and theoretical calculation clearly evidence the presence of a weak interaction between the Pd ion and the sulfur atom.

The investigated complexes generated active catalysts for the ethylene/methyl acrylate copolymerization under mild reaction conditions of temperature and ethylene pressure by carrying out the catalysis in two different solvents, dichloromethane or trifluoroethanol. Productivities as high as 79 kg CP/mol Pd and MA incorporations up to 8% have been achieved. The produced macromolecules have M_n values in the range 5−30 kDa and the degree of branching between 87 and 120 branches per 1000 carbon atoms. NMR characterization of the macromolecules evidences that the acrylate is inserted both in the main chain and at the end of the branches in a ratio that ranges from 9:91 to 45:55 moving from dichloromethane to trifluoroethanol as a solvent for the catalysis and varying the N−S ligand.

Some remarkable differences with respect to the well-known typical reactivity of the Pd-α-diimine catalysts emerged from in situ NMR monitoring of the reactions of both the parent compound [Pd(Me)(**MeDAB**)(MeCN)][PF_6] **1** and one of the complexes with N−S, [Pd(Me)(**MeDAB**)($\mathbf{S}^{Ph}$)][PF_6] $\mathbf{1S}^{Ph}$, performed either in CD_2Cl_2 or in TFE-d_3 at room temperature, i.e.

https://doi.org/10.1021/acscatal.1c05326
ACS Catal. 2022, 12, 3430−3443

(i) a four-membered metallacycle was detected during the reaction of **1** with MA in CD_2Cl_2, in addition to the usual six- and five-membered palladacycles;
(ii) in contrast, the same experiment performed in TFE-d_3 resulted in the formation of an unprecedented open-chain intermediate, having both the organic fragment, deriving from the migratory insertion of MA into the Pd−Me bond, and the acetonitrile coordinated to palladium, in addition to the expected six-membered palladacycle; and
(iii) the abovementioned open-chain intermediate was also identified as a novel catalyst resting state during the reaction of **1** with MA and ethylene in TFE-d_3.

These results are in agreement with both reactivity studies and DFT calculations performed on $\mathbf{1S^{Ph}}$, pointing out that the N−S ligand remains in close proximity to the palladium ion favoring the formation of the open-chain intermediate instead of the expected six-membered metallacycle. The open-chain intermediate is responsible for trapping the polar monomer into the main chain.

This result might open the way to the discovery of new, efficient catalytic systems for the synthesis of functionalized polyolefins including polar vinyl monomers for which copolymerization via Pd-α-diimine catalysts had not been possible till date.

■ ASSOCIATED CONTENT

Supporting Information

The Supporting Information is available free of charge at https://pubs.acs.org/doi/10.1021/acscatal.1c05326.

Experimental procedures; NMR characterization of ligands, complexes, and polymers; catalytic data; X-ray characterization of complexes; NMR in situ studies; and DFT calculation (PDF)
Data ca59-06 (CIF)
Data dmr5-05 (CIF)
SI DFT (XYZ)

Accession Codes

CCDC 2117787 for $\mathbf{1S^{Ph}}$ and 2117786 for $\mathbf{1S^{Me}}$ contain the supplementary crystallographic data for this paper.

■ AUTHOR INFORMATION

Corresponding Author

Barbara Milani − *Dipartimento di Scienze Chimiche e Farmaceutiche, Università di Trieste, 34127 Trieste, Italy;* orcid.org/0000-0002-4466-7566; Email: milaniba@units.it

Authors

Chiara Alberoni − *Dipartimento di Scienze Chimiche e Farmaceutiche, Università di Trieste, 34127 Trieste, Italy*

Massimo C. D'Alterio − *Dipartimento di Chimica e Biologia "A. Zambelli", Università di Salerno, I-84084 Fisciano, SA, Italy*

Gabriele Balducci − *Dipartimento di Scienze Chimiche e Farmaceutiche, Università di Trieste, 34127 Trieste, Italy;* orcid.org/0000-0002-0007-0880

Barbara Immirzi − *Istituto per i Polimeri, Compositi e Biomateriali, Consiglio Nazionale delle Ricerche, 80078 Pozzuoli, NA, Italy*

Maurizio Polentarutti − *Elettra − Sincrotrone Trieste, Trieste 34149, Italy*

Claudio Pellecchia − *Dipartimento di Chimica e Biologia "A. Zambelli", Università di Salerno, I-84084 Fisciano, SA, Italy;* orcid.org/0000-0003-4358-1776

Complete contact information is available at: https://pubs.acs.org/10.1021/acscatal.1c05326

Funding

Università degli Studi di Trieste (B.M., G.B., and C.A.: FRA 2021).

Notes

The authors declare no competing financial interest.

■ ACKNOWLEDGMENTS

This work was supported by Università degli Studi di Trieste (B.M., G.B., and C.A.: FRA 2021). The Ph.D. fellowship of C.A. was supported by FSE-PO 2014/2020 and Regione FVG, Program 89/19.

■ REFERENCES

(1) Hees, T.; Zhong, F.; Stürzel, M.; Mülhaupt, R. Tailoring Hydrocarbon Polymers and All-Hydrocarbon Composites for Circular Economy. *Macromol. Rapid Commun.* **2019**, *40*, No. 1800608.
(2) Luckham, S. L. J.; Nozaki, K. Toward the Copolymerization of Propylene with Polar Comonomers. *Acc. Chem. Res.* **2021**, *54*, 344−355.
(3) Vollmer, I.; Jenks, M. J. F.; Roelands, M. C. P.; White, R. J.; van Harmelen, T.; de Wild, P.; van der Laan, G. P.; Meirer, F.; Keurentjes, J. T. F.; Weckhuysen, B. M. Beyond Mechanical Recycling: Giving New Life to Plastic Waste. *Angew. Chem., Int. Ed.* **2020**, *59*, 15402−15423.
(4) Nakamura, A.; Ito, S.; Nozaki, K. Coordination-Insertion Copolymerization of Fundamental Polar Monomers. *Chem. Rev.* **2009**, *109*, 5215−5244.
(5) Carrow, B. P.; Nozaki, K. Transition-Metal-Catalyzed Functional Polyolefin Synthesis: Effecting Control through Chelating Ancillary Ligand Design and Mechanistic Insights. *Macromolecules* **2014**, *47*, 2541−2555.
(6) Tan, C.; Chen, C. Emerging Palladium and Nickel Catalysts for Copolymerization of Olefins with Polar Monomers. *Angew. Chem., Int. Ed.* **2019**, *58*, 7192−7200.
(7) Keyes, A.; Basbug Alhan, H. E.; Ordonez, E.; Ha, U.; Beezer, D. B.; Dau, H.; Liu, Y.-S.; Tsogtgerel, E.; Jones, G. R.; Harth, E. Olefins and Vinyl Polar Monomers: Bridging the Gap for Next Generation Materials. *Angew. Chem., Int. Ed.* **2019**, *58*, 12370−12391.
(8) Franssen, N. M. G.; Reek, J. N. H.; de Bruin, B. Synthesis of functional 'polyolefins': state of the art and remaining challenges. *Chem. Soc. Rev.* **2013**, *42*, 5809−5832.
(9) Johnson, L. K.; Mecking, S.; Brookhart, M. Copolymerization of ethylene and propylene with functionalized vinyl monomers by palladium(II) catalysts. *J. Am. Chem. Soc.* **1996**, *118*, 267−268.
(10) Mecking, S.; Johnson, L. K.; Wang, L.; Brookhart, M. Mechanistic studies of the palladium-catalyzed copolymerization of ethylene and alpha-olefins with methyl acrylate. *J. Am. Chem. Soc.* **1998**, *120*, 888−899.
(11) Drent, E.; van Dijk, R.; van Ginkel, R.; van Oort, B.; Pugh, R. I. Palladium catalysed copolymerisation of ethene with alkylacrylates: polar comonomer built into the linear polymer chain. *Chem. Commun.* **2002**, 744−745.
(12) Kochi, T.; Yoshimura, K.; Nozaki, K. Synthesis of anionic methylpalladium complexes with phosphine-sulfonate ligands and their activities for olefin polymerization. *Dalton Trans.* **2006**, *38*, 25−27.
(13) Guironnet, D.; Roesle, P.; Runzi, T.; Gottker-Schnetmann, I.; Mecking, S. Insertion Polymerization of Acrylate. *J. Am. Chem. Soc.* **2009**, *131*, 422−423.

(14) Nakamura, A.; Anselment, T. M. J.; Claverie, J.; Goodall, B.; Jordan, R. F.; Mecking, S.; Rieger, B.; Sen, A.; Van Leeuwen, P.; Nozaki, K. Ortho-Phosphinobenzenesulfonate: A Superb Ligand for Palladium-Catalyzed Coordination-Insertion Copolymerization of Polar Vinyl Monomers. *Acc. Chem. Res.* **2013**, *46*, 1438−1449.
(15) Wang, F.; Chen, C. A continuing legend: the Brookhart-type α-diimine nickel and palladium catalysts. *Polym. Chem.* **2019**, *10*, 2354−2369.
(16) Chen, Z.; Brookhart, M. Exploring Ethylene/Polar Vinyl Monomer Copolymerizations Using Ni and Pd α-Diimine Catalysts. *Acc. Chem. Res.* **2018**, *51*, 1831−1839.
(17) Dai, S.; Zhou, S.; Zhang, W.; Chen, C. Systematic Investigations of Ligand Steric Effects on α-Diimine Palladium Catalyzed Olefin Polymerization and Copolymerization. *Macromolecules* **2016**, *49*, 8855−8862.
(18) Mitsushige, Y.; Carrow, B. P.; Ito, S.; Nozaki, K. Ligand-controlled insertion regioselectivity accelerates copolymerisation of ethylene with methyl acrylate by cationic bisphosphine monoxide-palladium catalysts. *Chem. Sci.* **2016**, *7*, 737−744.
(19) Contrella, N. D.; Sampson, J. R.; Jordan, R. F. Copolymerization of Ethylene and Methyl Acrylate by Cationic Palladium Catalysts That Contain Phosphine-Diethyl Phosphonate Ancillary Ligands. *Organometallics* **2014**, *33*, 3546−3555.
(20) Sui, X.; Dai, S.; Chen, C. Ethylene Polymerization and Copolymerization with Polar Monomers by Cationic Phosphine Phosphonic Amide Palladium Complexes. *ACS Catal.* **2015**, *5*, 5932−5937.
(21) Zhang, W.; Waddell, P. M.; Tiedemann, M. A.; Padilla, C. E.; Mei, J.; Chen, L.; Carrow, B. P. Electron-rich metal cataions enable synthesis of high molecular weight, linear functional polyethylenes. *J. Am. Chem. Soc.* **2018**, *140*, 8841−8850.
(22) Nakano, R.; Nozaki, K. Copolymerization of Propylene and Polar Monomers Using Pd/IzQO Catalysts. *J. Am. Chem. Soc.* **2015**, *137*, 10934−10937.
(23) Tao, W.; Akita, S.; Nakano, R.; Ito, S.; Hoshimoto, Y.; Ogoshi, S.; Nozaki, K. Copolymerisation of ethylene with polar monomers by using palladium catalysts bearing an N-heterocyclic carbene-phosphine oxide bidentate ligand. *Chem. Commun.* **2017**, *53*, 2630−2633.
(24) Takano, S.; Takeuchi, D.; Osakada, K.; Akamatsu, N.; Shishido, A. Dipalladium Catalyst for Olefin Polymerization: Introduction of Acrylate Units into the Main Chain of Branched Polyethylene. *Angew. Chem., Int. Ed.* **2014**, *53*, 9246−9250.
(25) Zhang, Y.; Wang, C.; Mecking, S.; Jian, Z. Ultrahigh Branching of Main-Chain-Functionalized Polyethylenes by Inverted Insertion Selectivity. *Angew. Chem., Int. Ed.* **2020**, *59*, 14296−14302.
(26) Zhang, Y.; Jian, Z. Comprehensive Picture of Functionalized Vinyl Monomers in Chain-Walking Polymerization. *Macromolecules* **2020**, *53*, 8858−8866.
(27) Saki, Z.; D'Auria, I.; Dall'Anese, A.; Milani, B.; Pellecchia, C. Copolymerization of Ethylene and Methyl Acrylate by Pyridylimino Ni(II) Catalysts Affording Hyperbranched Poly(ethylene-co-methyl acrylate)s with Tunable Structures of the Ester Groups. *Macromolecules* **2020**, *53*, 9294−9305.
(28) Zhai, F.; Solomon, J. B.; Jordan, R. F. Copolymerization of Ethylene with Acrylate Monomers by Amide-Functionalized α-Diimine Pd Catalysts. *Organometallics* **2017**, *36*, 1873−1879.
(29) Gong, Y.; Li, S.; Tan, C.; Kong, W.; Xu, G.; Zhang, S.; Liu, B.; Dai, S. π−π interaction effect in insertion polymerization with α-Diimine palladium systems. *J. Catal.* **2019**, *378*, 184−191.
(30) Dai, S.; Chen, C. Direct Synthesis of Functionalized High-Molecular-Weight Polyethylene by Copolymerization of Ethylene with Polar Monomers. *Angew. Chem., Int. Ed.* **2016**, *55*, 13281−13285.
(31) Zhang, Y.; Jian, Z. Polar Additive Triggered Branching Switch and Block Polyolefin Topology in Living Ethylene Polymerization. *Macromolecules* **2021**, *54*, 3191−3196.
(32) Chen, C. Designing catalysts for olefin polymerization and copolymerization: beyond electronic and steric tuning. *Nat. Rev. Chem.* **2018**, *2*, 6−14.
(33) Bourque, A. N.; Dufresne, S.; Skene, W. G. Thiophene-Phenyl Azomethines with Varying Rotational Barriers - Model Compounds for Examining Imine Fluorescence Deactivation. *J. Phys. Chem. C* **2009**, *113*, 19677−19685.
(34) Canil, G.; Rosar, V.; Dalla Marta, S.; Bronco, S.; Fini, F.; Carfagna, C.; Durand, J.; Milani, B. Unprecedented Comonomer Dependence of the Stereochemistry Control in Pd-Catalyzed CO/Vinyl Arene Polyketone Synthesis. *ChemCatChem* **2015**, *7*, 2255−2264.
(35) Rosar, V.; Dedeic, D.; Nobile, T.; Fini, F.; Balducci, G.; Alessio, E.; Carfagna, C.; Milani, B. Palladium complexes with simple iminopyridines as catalysts for polyketone synthesis. *Dalton Trans.* **2016**, *45*, 14609−14619.
(36) Dall'Anese, A.; Fiorindo, M.; Olivieri, D.; Carfagna, C.; Balducci, G.; Alessio, E.; Durand, J.; Milani, B. Pd-Catalyzed CO/Vinyl Arene Copolymerization: when the Stereochemistry is Controlled by the Comonomer. *Macromolecules* **2020**, *53*, 7783−7794.
(37) Rülke, R. E.; Delis, J. G. P.; Groot, A. M.; Elsevier, C. J.; Van Leeuwen, P. W. N. M.; Vrieze, K.; Goubitz, K.; Schenk, H. Insertion reactions involving palladium complexes with nitrogen ligands. 1. reactivity towards carbon monoxide of methylpalladium(II) complexes containing bidentate alpha-diimine ligands: crystal structures of four methylpalladium (II) and acylpalladium(II) complexes. *J. Organomet. Chem.* **1996**, *508*, 109−120.
(38) Bader, R. F. W. *Atoms in Molecules. A Quantum Theory*; Clarendon: Oxford, 1990.
(39) Bader, R. F. W.; Essén, H. The characterization of atomic interactions. *J. Chem. Phys.* **1984**, *80*, 1943−1960.
(40) Milani, B.; Anzilutti, A.; Vicentini, L.; Sessanta o Santi, A.; Zangrando, E.; Geremia, S.; Mestroni, G. Bis-chelated palladium(II) complexes with nitrogen-donor chelating ligands are efficient catalyst precursors for the CO/styrene copolymerization reaction. *Organometallics* **1997**, *16*, 5064−5075.
(41) Scarel, A.; Durand, J.; Franchi, D.; Zangrando, E.; Mestroni, G.; Milani, B.; Gladiali, S.; Carfagna, C.; Binotti, B.; Bronco, S.; Gragnoli, T. Trifluoroethanol: Key solvent for palladium-catalyzed polymerization reactions. *J. Organomet. Chem.* **2005**, *690*, 2106−2120.
(42) Rosar, V.; Montini, T.; Balducci, G.; Zangrando, E.; Fornasiero, P.; Milani, B. Palladium-Catalyzed Ethylene/Methyl Acrylate Co-Oligomerization: The Effect of a New Nonsymmetrical α-Diimine with the 1,4-Diazabutadiene Skeleton. *ChemCatChem* **2017**, *9*, 3402−3411.
(43) Dall'Anese, A.; Rosar, V.; Cusin, L.; Montini, T.; Balducci, G.; D'Auria, I.; Pellecchia, C.; Fornasiero, P.; Felluga, F.; Milani, B. Palladium-Catalyzed Ethylene/Methyl Acrylate Copolymerization: Moving from the Acenaphthene to the Phenanthrene Skeleton of α-Diimine Ligands. *Organometallics* **2019**, *38*, 3498−3511.
(44) Meduri, A.; Montini, T.; Ragaini, F.; Fornasiero, P.; Zangrando, E.; Milani, B. Palladium-Catalyzed Ethylene/Methyl Acrylate Cooligomerization: Effect of a New Nonsymmetric α-Diimine. *ChemCatChem* **2013**, *5*, 1170−1183.
(45) Allen, K. E.; Campos, J.; Daugulis, O.; Brookhart, M. Living Polymerization of Ethylene and Copolymerization of Ethylene/Methyl Acrylate Using "Sandwich" Diimine Palladium Catalysts. *ACS Catal.* **2015**, *5*, 456−464.
(46) Ó Máille, G. M.; Dall'Anese, A.; Grossenbacher, P.; Montini, T.; Milani, B.; Albrecht, M. Modulation of N∧N′-bidentate chelating pyridyl−pyridylidene amide ligands offers mechanistic insights into Pd-catalysed ethylene/methyl acrylate copolymerisation. *Dalton Trans.* **2021**, *50*, 6133−6145.
(47) Milani, B.; Marson, A.; Zangrando, E.; Mestroni, G.; Ernsting, J. M.; Elsevier, C. J. New monocationic methylpalladium(II) compounds with several bidentate nitrogen-donor ligands: synthesis, Characterisation and reactivity with CO. *Inorg. Chim. Acta* **2002**, *327*, 188−201.

https://doi.org/10.1021/acscatal.1c05326
ACS Catal. 2022, 12, 3430−3443